Bioinformatics analysis of necroptosis-related lncRNAs and immune infiltration, and prediction of the prognosis of patients with esophageal carcinoma

XIAOYANG DUAN[1], HUAZHEN DU[2], MENG YUAN[3], LIE LIU[4], RONGFENG LIU[1] and JIAN SHI[1]

Departments of [1]Medical Oncology and [2]Emergency, The Fourth Hospital of Hebei Medical University, Shijiazhuang, Hebei 050000, P.R. China; [3]Department of Internal Medicine, University of Occupational and Environmental Health, Kitakyushu, Fukuoka 804-8550, Japan; [4]Graduate School, Hebei Medical University, Shijiazhuang, Hebei 050017, P.R. China

Received November 21, 2022; Accepted April 21, 2023

DOI: 10.3892/etm.2023.12030

Abstract. Esophageal carcinoma (ESCA) is one of the most common malignancies in the world, and has high morbidity and mortality rates. Necrosis and long noncoding RNAs (lncRNAs) are involved in the progression of ESCA; however, the specific mechanism has not been clarified. The aim of the present study was to investigate the role of necrosis-related lncRNAs (nrlncRNAs) in patients with ESCA by bioinformatics analysis, and to establish a nrlncRNA model to predict ESCA immune infiltration and prognosis. To form synthetic matrices, ESCA transcriptome data and related information were obtained from The Cancer Genome Atlas. A nrlncRNA model was established by coexpression, univariate Cox (Uni-Cox), and least absolute shrinkage and selection operator analyses. The predictive ability of this model was evaluated by Kaplan-Meier, receiver operating characteristic (ROC) curve, Uni-Cox, multivariate Cox regression, nomogram and calibration curve analyses. A model containing eight nrlncRNAs was generated. The areas under the ROC curves for 1-, 3- and 5-year overall survival were 0.746, 0.671 and 0.812, respectively. A high-risk score according to this model could be used as an indicator for systemic therapy use, since the half-maximum inhibitory concentration values varied significantly between the high-risk and low-risk groups. Based on the expression of eight prognosis-related nrlncRNAs, the patients with ESCA were regrouped using the 'ConsensusClusterPlus' package to explore potential molecular subgroups responding to immunotherapy. The patients with ESCA were divided into three clusters based on the eight nrlncRNAs that constituted the risk model: The most low-risk group patients were classified into cluster 1, and the high-risk group patients were mainly concentrated in clusters 2 and 3. Survival analysis showed that Cluster 1 had a better survival than the other groups (P=0.016). This classification system could contribute to precision treatment. Furthermore, two nrlncRNAs (LINC02811 and LINC00299) were assessed in the esophageal epithelial cell line HET-1A, and in the human esophageal cancer cell lines KYSE150 and TE1. There were significant differences in the expression levels of these lncRNAs between tumor and normal cells. In conclusion, the present study suggested that nrlncRNA models may predict the prognosis of patients with ESCA, and provide guidance for immunotherapy and chemotherapy decision making. Furthermore, the present study provided strategies to promote the development of individualized and precise treatment for patients with ESCA.

Introduction

Esophageal carcinoma (ESCA) is one of the most common cancers in the world. According to statistics, there were over 600,000 new cases of esophageal cancer worldwide and over 540,000 related deaths in 2020; it ranked 7th in incidence and 6th in mortality among all cancers (1). The tissue subtypes of esophageal cancer are divided into esophageal squamous cell carcinoma (ESCC) and esophageal adenocarcinoma (EAC), of which ESCC is the main subtype. The incidence and distribution of histological types vary according to geographic location. ESCC accounts for more than 90% of esophageal cancer cases in developing countries, and approximately 50% of new cases occur in China; its incidence is increasing each year (2,3). With the rapid development of medical technology, many methods are being used to treat ESCC, and these methods include surgery, chemotherapy, radiotherapy, and immune checkpoint inhibitor therapy.

However, the early symptoms of ESCC patients are not obvious, and the disease is typically in an advanced stage at diagnosis, which leads to a poor prognosis in ESCC patients; ESCC has a 5-year survival rate of only 14~22% (4-6). Esophageal cancer has become one of the deadliest cancers, mainly due to its high aggressiveness and low survival rate. Therefore, novel biomarkers of esophageal cancer are urgently

Correspondence to: Professor Jian Shi, Department of Medical Oncology, The Fourth Hospital of Hebei Medical University, 12 Jiankang Road, Shijiazhuang, Hebei 050000, P.R. China
E-mail: shijian6668@126.com

Key words: necroptosis, lncRNA, esophageal carcinoma, prognostic model, bioinformatics

required to facilitate early diagnosis, tumor-targeted drug development and ESCA prognosis prediction.

Necroptosis is a form of programmed inflammatory cell death that was first reported by Degterev *et al* (7). Necroptosis involves a phosphorylation signal mediated by serine/threonine protein kinase 1/3 (RIPK1/RIPK3). Necrosis shares a common pathway with apoptosis: the mixed lineage kinase domain protein (MLKL/pMLKL) pathway (8,9). This pattern involves necrotic cell death; the related morphological features include lysosomal membrane degradation, cytoplasmic vacuolation, plasma membrane disintegration, and finally, explosive cell rupture (10,11). In recent years, increasing evidence has shown that necroptosis plays an important role in tumorigenesis, metastasis, and the tumor immune response. It has been reported that activation of the necrosis-related genes RIPK1 and RIPK3 or necrosis-related signaling pathways is involved in the regulation of tumor cell metabolic biological processes and the tumor microenvironment (12-15). Studies have shown that necroptosis can not only promote the occurrence and development of cancer but also inhibit the occurrence and development of cancer, and its specific role depends on the type of tumor and its developmental stage. Low expression of RIPK3 facilitates resistance to necroptosis in some tumors, such as acute myeloid leukemia (16), chronic lymphocytic leukemia (17) and breast adenocarcinoma (18), and thus can readily promote tumor growth. However, high levels of phosphorylated MLKL have been shown to be associated with a poor prognosis in patients with colon cancer (19) and esophageal cancer (20). Necroptosis may play an important role in eliciting immunogenicity and promoting natural anticancer immune surveillance. Studies have shown that tumor cells undergo necroptosis to release IL-lα to activate dendritic cells (DCs). Activated DCs induce antitumor immune responses by producing the cytotoxic cytokine IL-12 and activating CD8+ T cells to eliminate cancer cells (21,22). Similarly, damage-associated molecular patterns (DAMPs) from necrotic tumor cells strongly induce the activation of antitumor CD8+ T cells (23). It has also been shown that NKT cells are involved in RIPK3-mediated antitumor immune responses, as the loss of RIPK3 impairs the activation of NKT cells to prevent tumor killing (24). All these findings suggest that necroptosis inhibits tumor initiation and progression. On the other hand, tumor cell metastasis is the main cause of death in cancer patients. Metastasis refers to the dissemination of individual tumor cells through the circulatory system to other distant organs for further growth. Necroptosis can promote tumor development and metastasis through a variety of mechanisms. Extravasation of tumor cells through the endothelium is an important step in metastatic spread. Tumor cells induce the necroptosis of endothelial cells by activating death receptor 6 (DR6 encoded by TNFRSF21), another member of the death receptor family, thereby promoting tumor cell extravasation and metastasis. In mice treated with Nec-1 or mice with endothelial cell-specific knockout of RIPK3 or MLKL, we observed a reduction in tumor cell-induced necroptosis of endothelial cells, which thereby reduced tumor cell extravasation and metastasis (25). In addition, metastasis also involves a complex interaction between cancer cells and the tumor microenvironment, which involves factors including immune cell infiltration and cytokine secretion. Necroptosis is a type of proinflammatory cell death, and the inflammatory response caused by necroptosis may lead to tumor metastasis. In pancreatic ductal adenocarcinoma (PDAC), RIPK3 knockout tumor cells undergo necroptosis and release soluble cytokines that bind to receptors on inflammatory cells; for example, cytokine SAP130 is released and binds its cognate receptor Mincle, thereby initiating an immunosuppressive tumor microenvironment and promoting the progression of PDAC (26). Therefore, studying necroptosis-related genes in tumor cells and their regulatory mechanisms is expected to reveal a target for ESCA therapy.

Long noncoding RNAs (lncRNAs) refer to noncoding RNAs with a length greater than 200 nucleotides that lack protein-coding ability and can play a variety of important biological roles in cells (27). It has been reported that lncRNAs participate in and exacerbate tumor inflammation and tumor microenvironment disorder and prevent tumor immune escape (28). LINC00680 promotes esophageal squamous cell carcinoma progression through the miR-423-5p/PAK6 axis. Knockdown of LINC00680 was found to inhibit ESCC cell proliferation, colony formation, migration and invasion *in vitro* and tumor growth *in vivo* (29). LncRNA ZEB2-AS1 is upregulated in ESCC tissues and cells vs. corresponding controls. It has been verified to promote the proliferation, migration and invasion of esophageal squamous cell carcinoma cells by modulating the miR-574-3p/HMGA2 axis (30). In addition, lncRNA necrosis-related factor (NRF) regulates cardiomyocyte necroptosis by targeting miR-873 and RIPK1/RIPK3 (31). Previous studies have reported that lncRNAs associated with necrosis can be used to predict the features of many tumors (including head and neck squamous cancer, gastric cancer, colon cancer and breast cancer) and their immune environment (32-35). However, the relationship between lncRNAs and necrosis in ESCA remains unclear and needs further investigation. Therefore, a prognostic risk model of necrosis-related lncRNAs (nrlncRNAs) was constructed in this study to predict the prognosis of ESCA patients and provide guidance for clinical diagnosis and treatment.

Materials and methods

Acquisition of transcriptome-level gene expression data and clinical data for patients with esophageal cancer. RNA sequencing-seq (RNA-seq) transcriptome data for patients with ESCA were downloaded from the TCGA-ESCA dataset (https://portal.gdc.cancer.gov/); the related samples included 11 normal samples and 161 ESCA tumor samples (last accessed: 10 May 2022). To reduce potential statistical bias in the sample analysis, patients with no OS data or short OS time (<30 days) were excluded, and patients in the TCGA-ESCA cohort were randomly divided into the training risk group and the test risk group with Strawberry Perl at a ratio of 1:1.

Identification of nrlncRNAs. According to previous studies, we downloaded the necroptosis gene set M24779.gmt from the Gene Set Enrichment Analysis (GSEA) website (http://www.gsea-msigdb.org/gsea/index.jsp) and further extracted 8 necroptosis-related genes and 59 other genes (36). Then, correlation analysis was performed for 67 necroptosis-related genes and differentially expressed lncRNAs in the combined

matrices via Strawberry Perl and R software. Then, nrlncRNAs were identified with the criteria of |Pearson R|>0.4 and P<0.001.

Establishment and validation of the risk signature according to nrlncRNAs in ESCA. Univariate Cox (Uni-Cox) regression was used to screen lncRNAs associated with prognosis with P<0.05. Then, LASSO Cox analysis was performed to screen nrlncRNAs by 10-fold cross-validation, and the risk model P-value was 0.05. The number of resamples was increased to more than 1,000 to prevent overfitting error. Finally, the previously defined formula Risk score=$\sum$(nrlncRNA^{i}) coefficient x (nrlncRNA^{i}) expression was used to establish the prognostic risk profiles with eligible nrlncRNAs. ESCA patients in the TCGA cohort were divided into a low-risk group and a high-risk group in accordance with the median risk score. Kaplan-Meier (KM) survival analysis and log-rank test were performed using the survival R package to analyze whether there were differences in OS in the low-risk group of ESCA patients. That survival curves cross over may affect the results of log-rank analysis. When survival curves cross over, we reanalyze this dataset by the two-stage test (R package: https://cran.r-project.org/web/packages/TSHRC/TSHRC.pdf). The chi-square test was used to analyze the relationship between the model and clinical features to assess the prognostic value of the established risk features. Receiver operating characteristic (ROC) curves (1-year, 3-year, and 5-year survival rates) and the area under the ROC curve (AUC) values were evaluated to demonstrate the validity of the prediction model and compare its performance to that of models based on other clinical characteristics. Nomogram analysis was carried out via Uni-Cox and Multi-Cox analyses to evaluate survival predictions.

Enrichment analysis of genes. The related gene set (KEGG.v7.4.symbols. GMT) was analyzed by GSEA software version 4.2.3. The top 5 pathways in the low- and high-risk groups were selected based on the criterion of P<0.05.

Assessment of immune factors and the tumor microenvironment. We downloaded all the data on TCGA tumor invasion estimates from the website http://timer.cistrome.org/. Then, a variety of methods, including the Wilcoxon signed-rank test and analyses with the limma, scales, ggplot2, ggtext, tidyverse and ggpubr R packages, were employed, consistent with a previous report (37). Moreover, the stromal score, immune score, and ESTIMATE score (stromal score + immune score) of each patient were calculated. Then, single-sample GSEA (ssGSEA) was used to score the infiltrating immune cells in ESCA, and their relative content was quantified by the 'GSVA' package. The immune cell scores and pathways scores for various groups are shown on multiple boxplots. Finally, we analyzed and explored the differences in immune functions, immune cell infiltration and checkpoint expression levels between the low- and high-risk groups via the ggpubr R package.

Association between the risk model and clinical treatment. According to half-maximal inhibitory concentration (IC50) data for ESCA from the Genomics of Drug Sensitivity in Cancer (GDSC) database (https://www.cancerrxgene.org/), we used the 'pRRophetic' package to compare the therapeutic response between the low-risk and high-risk groups (38). This study focused on the analysis and comparison of the response to 48 commonly used chemotherapy drugs. When the P-value was less than 0.05, the IC50 values of the low-risk group and high-risk group were considered to be significantly different according to the Wilcoxon rank sum test.

Cluster analysis of prognostic nrlncRNAs. We evaluated the expression of nrlncRNAs related to prognosis using the 'ConsensusClusterPlus' package and assessed their ability to predict the response of ESCA patients to immunotherapy (39). Subsequently, K-M survival analysis, principal component analysis (PCA), and t-distributed stochastic neighbor embedding (t-SNE) were carried out with the Rtsne R package. Additionally, analyses of immune features and drug susceptibility were performed were performed with the GSVA and the pRRophetic R packages.

Reverse transcription-quantitative polymerase chain reaction (RT-qPCR). The esophageal epithelial cell line HET-1A and human esophageal cancer cell lines KYSE150 and TE1 were provided by the Research Center of the Fourth Hospital of Hebei Medical University. Total RNA of cells was extracted and purified using the TransZol Up Plus RNA Kit (TransGen Biotech, Beijing, China) according to the manufacturer's instructions. Total RNA was used to synthesize cDNA via the lnRcute lncRNA First-Strand cDNA kit (TIANGER, China). BlasTaq 2X qPCR Master Mix (Ab, China) was used for the PCR amplification process. All experimental procedures were carried out according to the commercial instructions. Because the AC090912.2, AC244197.2, AL158166.1, AC079684.1, AP003696.1, and AC026741.1 products may be artifacts or may not correspond to gene annotations, six gene primer pairs were designed for verification. Primers for LINC02811 and LINC00299 were designed and validated by PCR in three types of esophageal cells. The primer sequences for PCR amplification were as follows: LINC02811, forward: 5'-TTGGCACACTTAGCAAGGACTGAC-3', reverse: 5'-CTTCTGCCTCATTTCTGTCCTCCAC-3'; and LINC00299, forward: 5'-TCTGAAGTCACCTGCCCTATCTGG-3', reverse: 5'-TCCACTTGCCACTGCTTGCTTATC-3'. Each condition was replicated three times, and the quantitative analysis of gene expression was calculated by the $2^{-\Delta\Delta Cq}$ method. GAPDH was used as the internal control. The differences in LINC02811 and LINC00299 expression among HET-1A, KYSE150 and TE1 were assessed by a one-way ANOVA and Bonferroni correction post hoc test. GraphPad Prism (version 8.0.2) was applied to create the graphs.

Statistical analysis. All statistical evaluations utilized R (version 4.2.0). For each analysis, P<0.05 confirmed statistical significance. Univariate/multivariate Cox proportional hazard regression analyses were used for constructing a necroptosis-associated lncRNA model used as a predictive risk model. Chi-squared test was used to assess the medical features between different study groups. The log-rank test and Kaplan-Meier (KM) survival analysis was used to compare the differences in OS between low- and high-risk

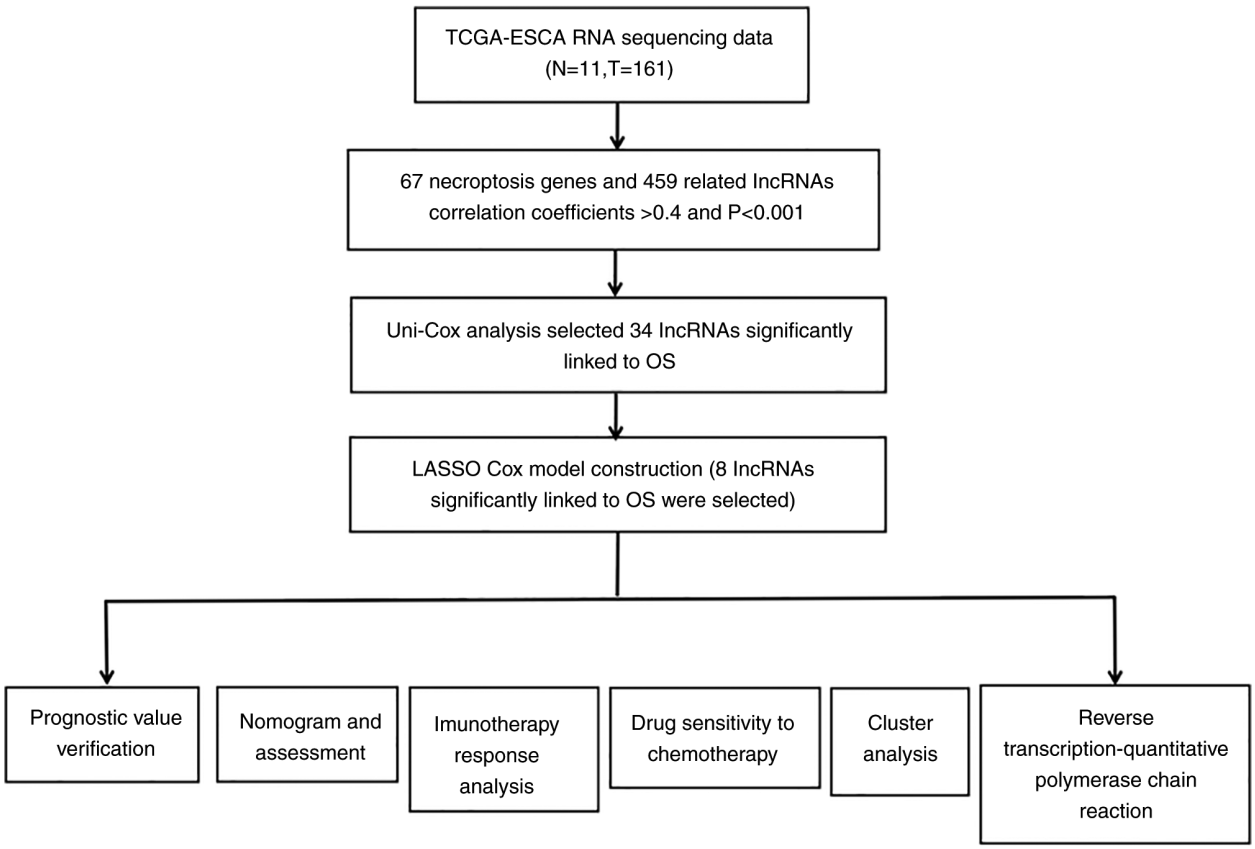

Figure 1. Flow diagram of the study. TCGA-ESCA, The Cancer Genome Atlas-esophageal carcinoma; Uni-Cox, univariate Cox; LASSO, least absolute shrinkage and selection operator.

groups. The survival receiver operating characteristic (ROC) curves and their areas under the curves (AUCs) were used to assess the efficacy of prediction, comparing with other clinical characteristics. Kruskal-Wallis test followed by Dunn's post hoc test was used to analyze the association between clusters, immune factors and the TME, and to compare drug susceptibility. Wilcoxon rank sum test was used to analyze the difference in IC_{50} values between the low-risk and high-risk groups. The relative expression of each gene was calculated and compared using the $2^{-\Delta\Delta Cq}$ method, and was analyzed by one-way ANOVA and Bonferroni correction. GraphPad Prism (version 8.0.2) was applied to create the graphs (*P<0.01, **P<0.001 and ***P<0.0001). Experiments were repeated three times.

Results

Analysis of nrlncRNAs in ESCA patients. The detailed flow diagram of the study design is shown in Fig. 1. The transcriptome data of ESCA downloaded from the TCGA included data for 11 normal samples and 161 ESCA tumor samples. According to the GTF file, the mRNAs and lncRNAs were distinguished in the transcriptome data. The data showed that 67 necrosis-associated genes were differentially expressed in normal and tumor samples. In addition, we finally obtained 459 nrlncRNAs, of which 103 were downregulated and 356 were upregulated based on the criteria of |log2-fold fold change (FC)|>1 and P<0.05. As shown in Fig. 2A, the analysis revealed the interaction relationship between genes and lncRNAs via a network diagram. A heatmap (Fig. 2B) and volcano plot (Fig. 2C) were used to reflect the differential expression of nrlncRNAs between normal and tumor samples.

Construction and verification of the nrlncRNA risk model. Uni-Cox regression analysis showed that 34 nrlncRNAs were associated with overall survival (OS) (all P<0.05), as shown in Fig. 2D (Uni-Cox forest map) and Fig. 2E (heatmap). For ESCA patients, 23 nrlncRNAs were identified as indicators of a poor prognosis (hazard ratio, HR>1); however, the remaining nrlncRNAs were favorable prognostic factors.

To avoid overfitting the prognostic model, the 34 nrlncRNAs were analyzed by LASSO regression analysis to establish prognostic variables. As shown in Fig. 2G and H, 8 nrlncRNAs were selected to develop the prognostic model according to nrlncRNA expression and the Multi-Cox regression analysis results. Additionally, the Sankey diagram analysis, as shown in Fig. 2F, revealed that all 34 nrlncRNAs were upregulated in ESCA patients.

The risk score formula was as follows: Risk score=(2.79718675565941 x LINC00299 expression)-(1.73124557102057 x AC090912.2 expression)-(2.81846794900141 x AC244197.2 expression)+(0.810897179352003 x AL158166.1 expression)+(0.90494089310592 x AC079684.1 expression)+(2.58956796584768 x AP003696.1expression)+

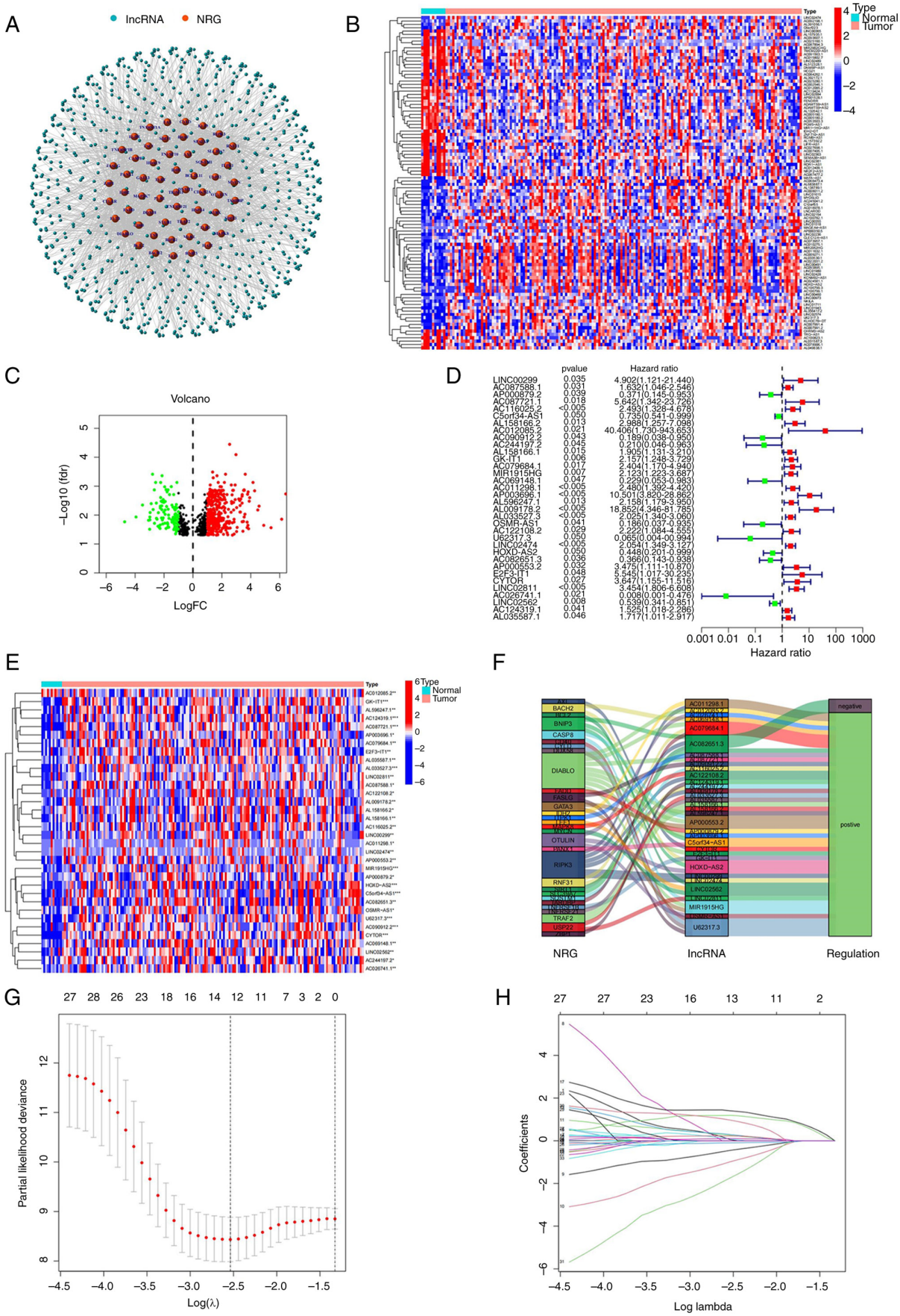

Figure 2. Identification and extraction of nrlncRNAs from the TCGA-ESCA dataset. (A) The network between genes and nrlncRNAs. (B) Heatmap of differentially expressed nrlncRNAs. (C) Volcano plot of differentially expressed nrlncRNAs. (D) Uni-Cox analysis of prognostic factors. (E) Expression profile heatmap of prognostic nrlncRNAs. (F) Sankey diagram of necroptosis-related genes and nrlncRNAs. (G) The 10-fold cross-validation for variable selection in the LASSO model. (H) The LASSO coefficient profile of 34 nrlncRNAs. TCGA-ESCA, The Cancer Genome Atlas-esophageal carcinoma; nrlncRNAs, necrosis-related lncRNAs; Uni-Cox, univariate Cox; LASSO, least absolute shrinkage and selection operator.

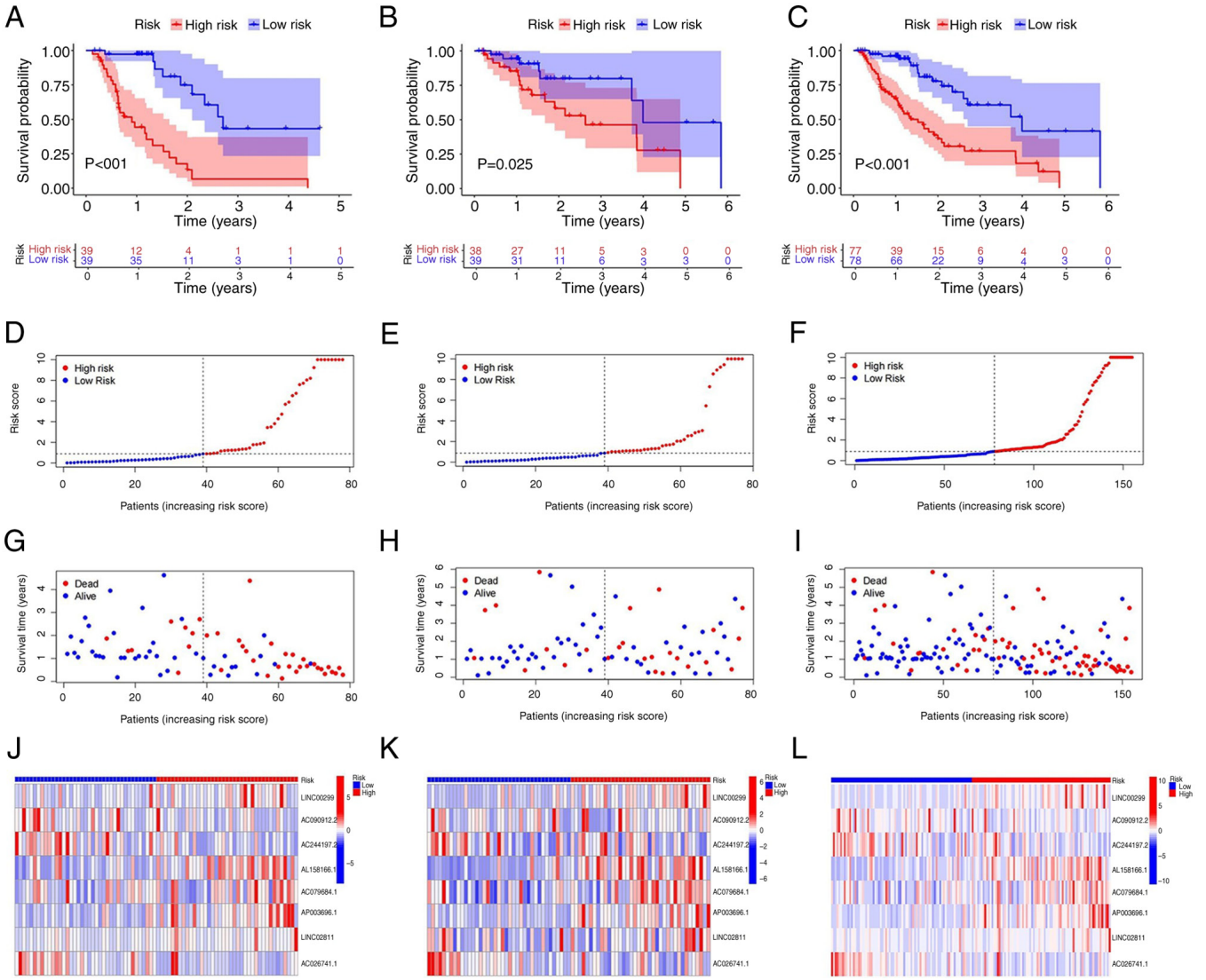

Figure 3. Prognostic value of the 8 signature nrlncRNAs in the training, testing, and entire datasets. (A-C) K-M survival curves of the OS probability of patients between low- and high-risk groups in (A) training group, (B) testing group and (C) entire group, respectively. (D-F) Demonstration of the nrlncRNA model based on the risk score in (D) training group, (E) testing group and (F) entire group, respectively. (G-I) Survival time and survival status between the low- and high-risk groups in (G) training group, (H) testing group and (I) entire group, respectively. (J-L) Heatmap of the expression of 8 lncRNAs in (J) training group, (K) testing group and (L) entire group, respectively. K-M, Kaplan-Meier; nrlncRNAs, necrosis-related lncRNAs.

(1.52401713479381 x LINC02811 expression)-(5.43761185912726 x AC026741.1 expression).

Based on the median risk score, the ESCA patients were divided high and low risk groups and then divided into training and testing groups. A total of 155 ESCA patients were enrolled, including 77 with high risk scores and 78 with low risk scores. In the training group, there were 39 patients each in the high risk and low risk subgroups. In the test group, there were 38 patients with high risk scores and 39 patients with low risk scores (Fig. 3A-C). Furthermore, comparison of the survival status, survival time and related lncRNA expression levels among these groups (Fig. 3D-L) suggested that the high-risk group had a poor prognosis.

Additionally, this risk score had high predictive efficiency in patients grouped by for age (Fig. 4A and B), sex (Fig. 4C and D), stage I-II (Fig. 4E), T stage (Fig. 4F and G), N stage (Fig. 4H and I) and M stage (Fig. 4J). For the different subgroups, the OS of the ESCA patients in the low-risk group was obviously longer than that of the patients in the high-risk group. These results suggest that the predictive signature can also predict the prognosis of ESCA patients in all subgroups based on age, sex, T stage and N stage and in the stage I-II and M0 stage subgroups. The area under the ROC curve (AUC) value of the risk model was 0.746, as shown in Fig. 4K, and this value was obviously higher than that of the model based on clinical characteristics, including age (0.545), sex (0.492), and stage (0.665; Fig. 4L).

The ability of the model to predict prognosis was evaluated independent of clinical characteristics such as age, sex and stage. As shown in Fig. 5A and B, Uni-Cox regression and multi-Cox regression showed that the HR values of the risk score were 3.594 (95% CI: 1.954 to 6.610) and 2.790 (95% CI: 1.482 to 5.252), respectively. Moreover, the HR values for disease stage were 2.703 (95% CI: 1.846 to 3.958) in the Uni-Cox regression analysis and 2.302 (95% CI: 1.523 to 3.481) in the Multi-Cox regression analysis, indicating that

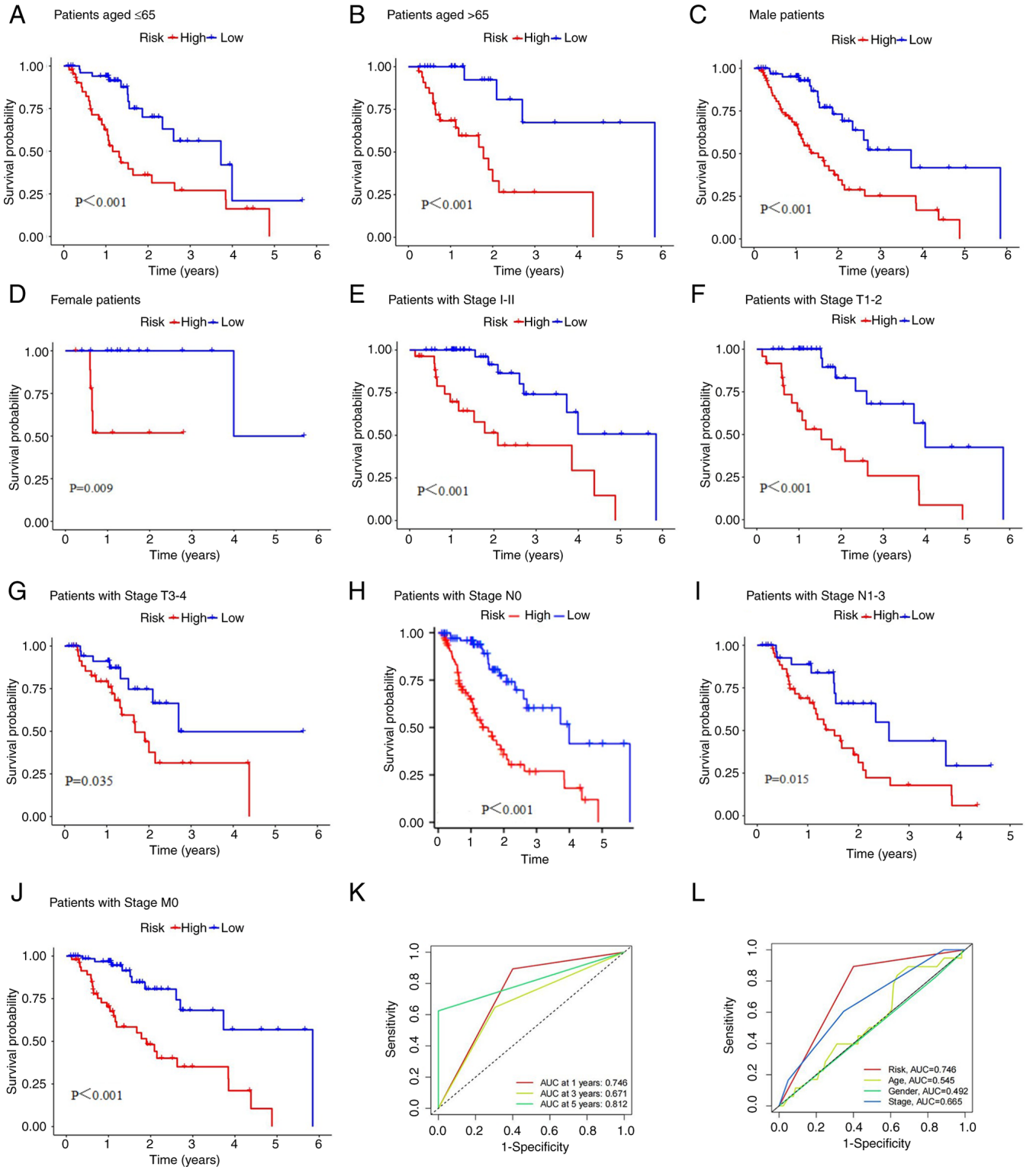

Figure 4. K-M survival curves of low- and high-risk groups in the entire dataset. (A) Patients aged ≤65, (B) patients aged >65, (C) male patients, (D) female patients, (E) patients with Stage I-II, (F) patients with Stage T1-2, (G) patients with Stage T3-4, (H) patients with Stage N0, (I) patients with Stage N1-3 and (J) patients with Stage M0. (K) 1-, 3-, and 5-year ROC curves of the entire dataset. (L) ROC curves of the risk score and clinicopathologic features such as age, sex, and stage. K-M, Kaplan-Meier; ROC, receiver operating characteristic.

stage, as an independent prognostic parameter, seems to be the main factor affecting prognosis.

Based on the risk score and independent clinical factors, a nomogram was constructed to predict the 1-, 3-, and 5-year survival rates of ESCA patients (Fig. 5C). Calibration plots confirmed the nomogram predictions had excellent concordance with the actual observations (Fig. 5D).

Gene enrichment analysis. To investigate the function of lncRNAs differentially expressed between the low- and

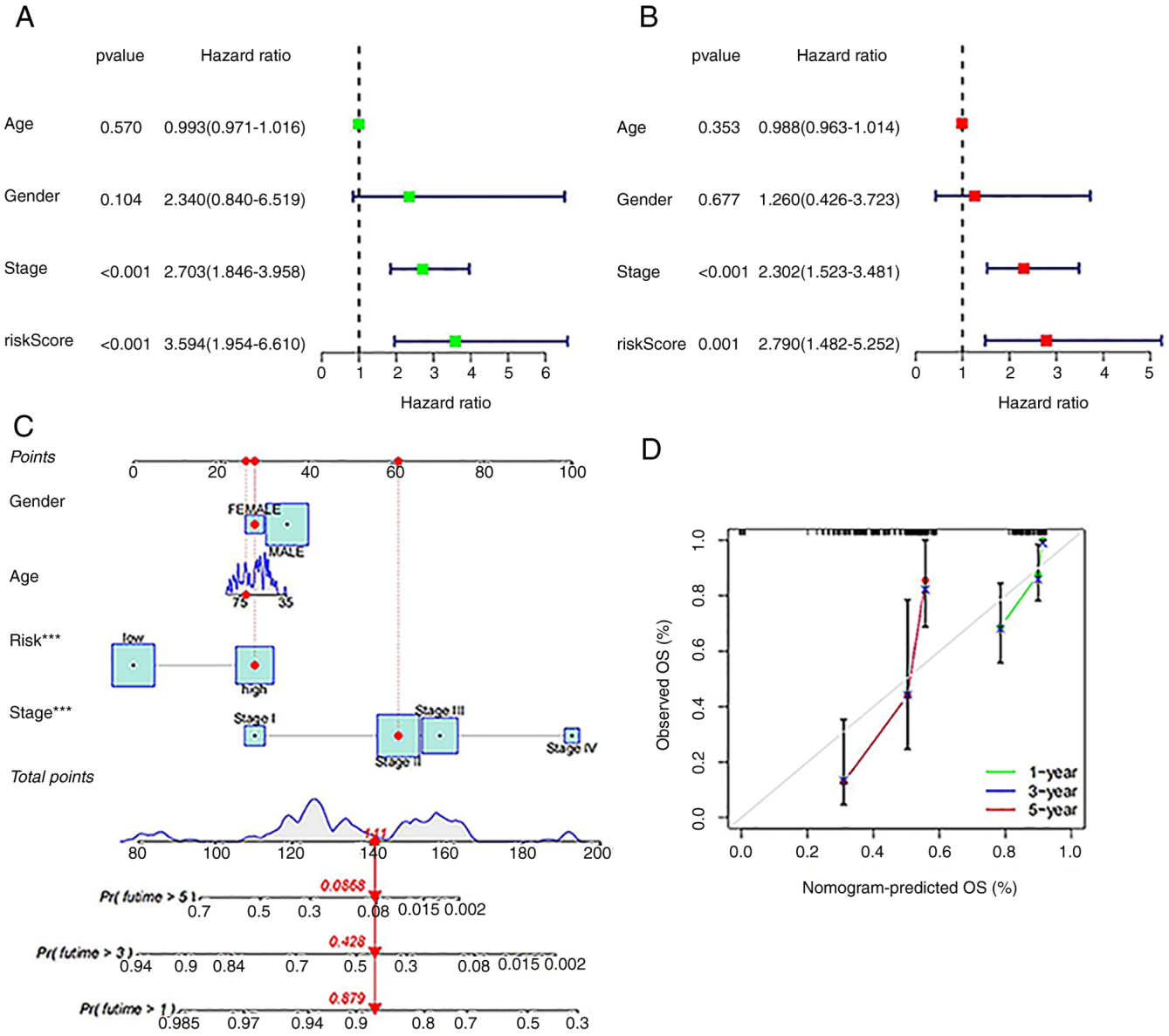

Figure 5. Nomogram and assessment of the risk model. (A and B) Uni-Cox and Multi-Cox analyses of clinical factors and risk score with OS. (C) Nomogram for predicting overall survival. (D) The calibration curves for 1-, 3-, and 5-year OS. Uni-Cox, univariate Cox; Multi-Cox, multivariate Cox; OS, overall survival.

high-risk groups in the whole set, As shown in Fig. 6A we explored the Kyoto Encyclopedia of Genes and Genomes (KEGG) pathways enriched in genes upregulated or downregulated in the high-risk group. The top 5 KEGG pathways enriched in upregulated and downregulated genes were highly related to tumor infiltration and immune escape. The analysis of these 10 pathways showed that regardless of the FDR value, the P-value was less than 0.05.

Correlations of the risk score with tumor immunity and microenvironment features. The relationship between the risk score and immune cell infiltration or functions was further investigated according to the enrichment score, and we quantified the enrichment scores of single-sample GSEA for different immune cell subsets, related functions or pathways. The boxplot suggested that the high-risk group had more neutrophils and Th2 cells, while the low-risk group had more macrophages and NK cells. There was no statistically significant difference in related immune functions between the two groups (Fig. 6B). We also found no significant differences in matrix scores, immune scores and ESTIMATE scores between the two groups (Fig. 6C).

Furthermore, as shown in Fig. 6D, we found that most of the immune checkpoints (TNFRSF18, BTNL2, CD276, CD40, CD86, CD44, and TNFSF18) showed greater activation in the low-risk group than in the other risk groups.

Clinical treatment response of the risk groups. The potential effective therapeutic drugs in the high-risk group were predicted by comparing the IC50 values of drugs in the low- and high-risk groups according to the pRRophetic method. As shown in Fig. 6E, we found that 48 chemotherapies or targeted drugs relevant to ESCA therapy showed lower IC50 values in the high-risk group.

Cluster analysis of prognostic nrlncRNAs. To further analyze the immune microenvironment and response of

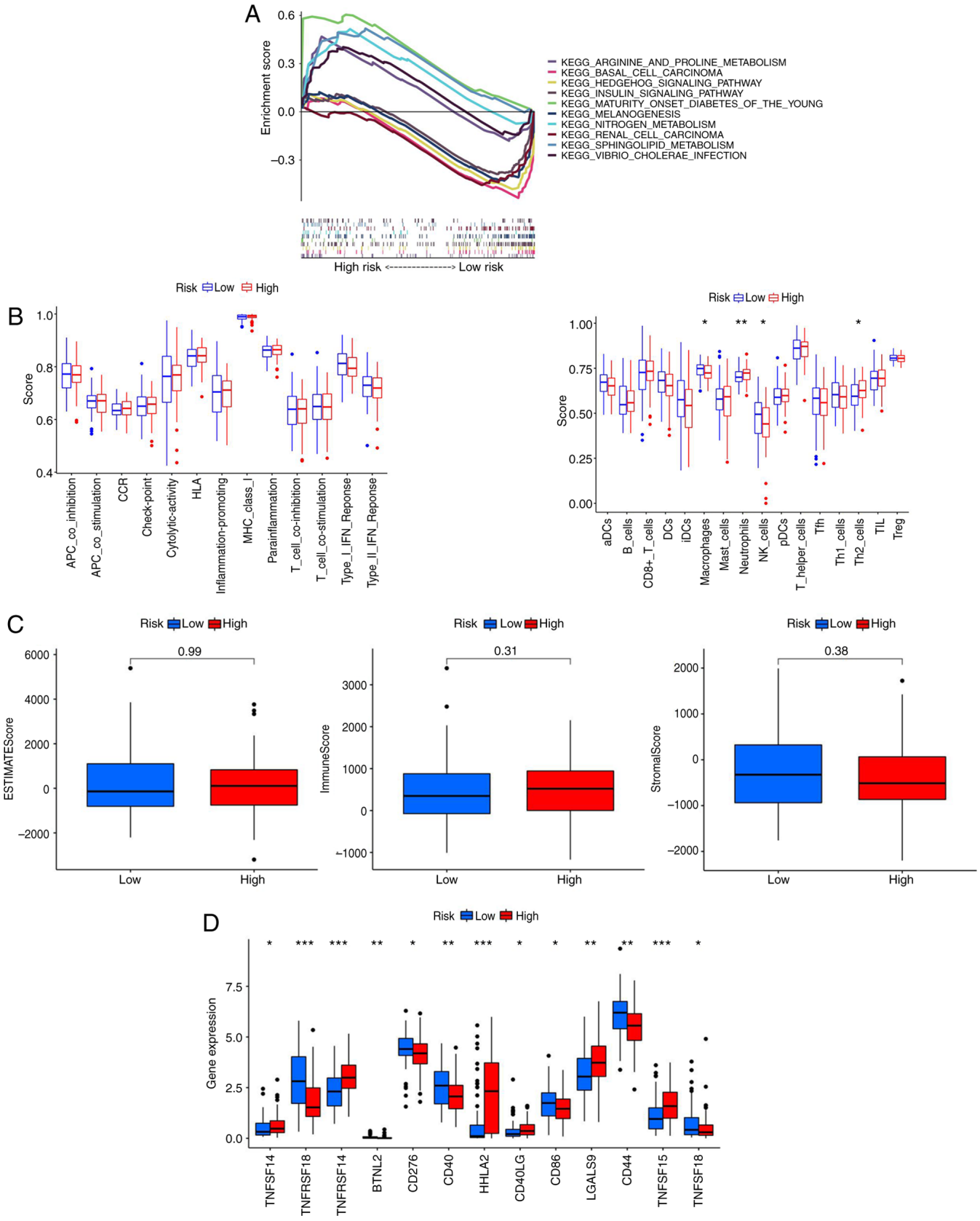

Figure 6. Contined.

different tumor subtypes, the clusters of ESCA patients were regrouped. As shown in Fig. 7A, we ultimately used the 'ConsensusClusterPlus' package to divide patients into 3 clusters based on the 8 nrlncRNAs that constituted the risk model. Moreover, as shown in the Sankey diagram (Fig. 7B), most low-risk group patients (blue) were classified into cluster 1. On the other hand, high-risk group patients were mainly concentrated in cluster 2 and cluster 3.

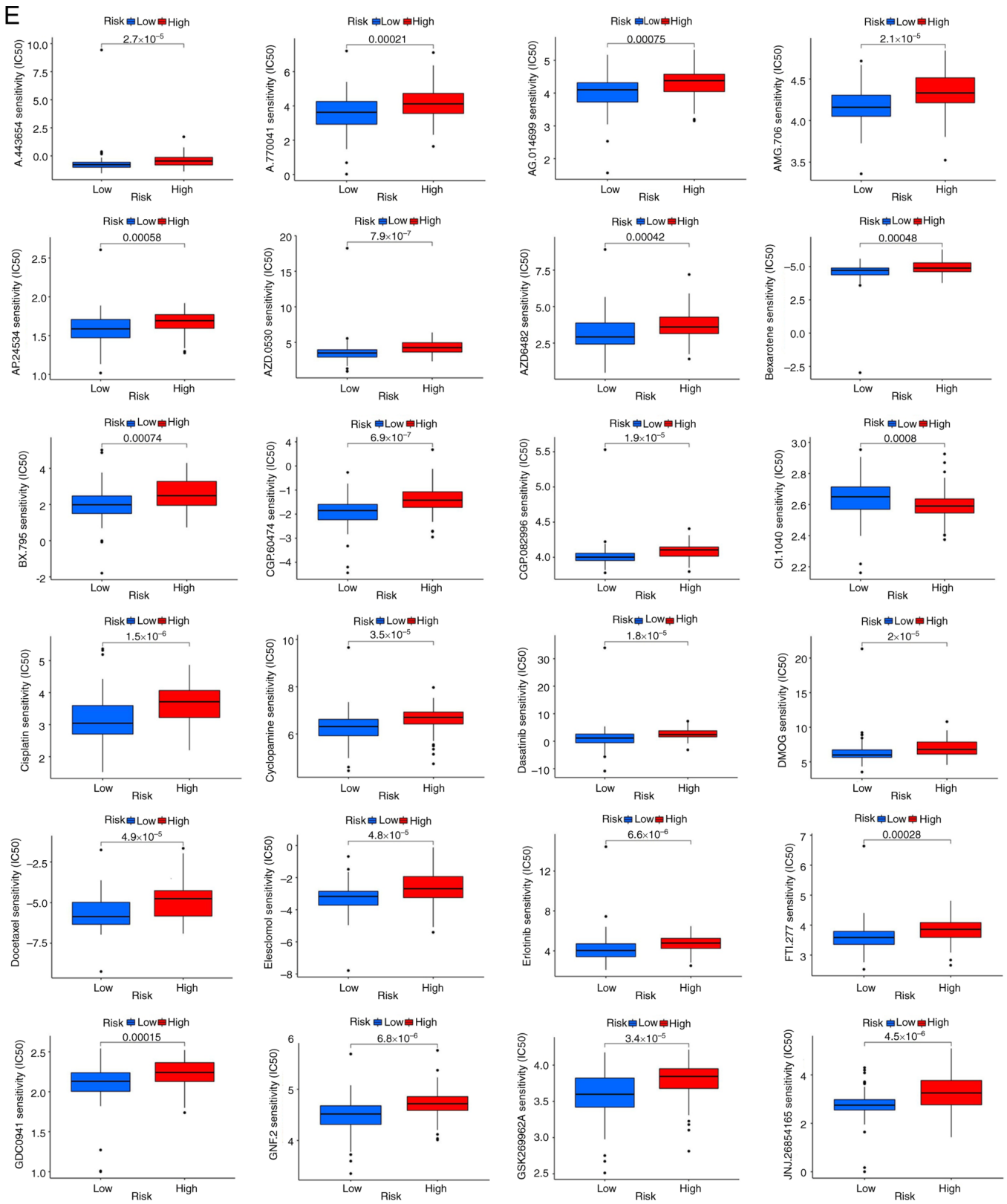

Figure 6. Contined.

Among them, cluster 1 had a better OS (P=0.016) than cluster 2 and cluster 3 (Fig. 7C). As shown in Fig. 7D, the PCA results showed that PCs in the risk group and cluster were different, and clusters could be clearly distinguished through t-SNE verification (Fig. 7E). We also analyzed the correlation between cluster, immune factors and the TME by the Kruskal-Wallis test followed by Dunn's post hoc test. However, from the results of the boxplot, there were no significant differences in the stromal score, immune score and ESTIMATE score among the three groups (Fig. 7F). As

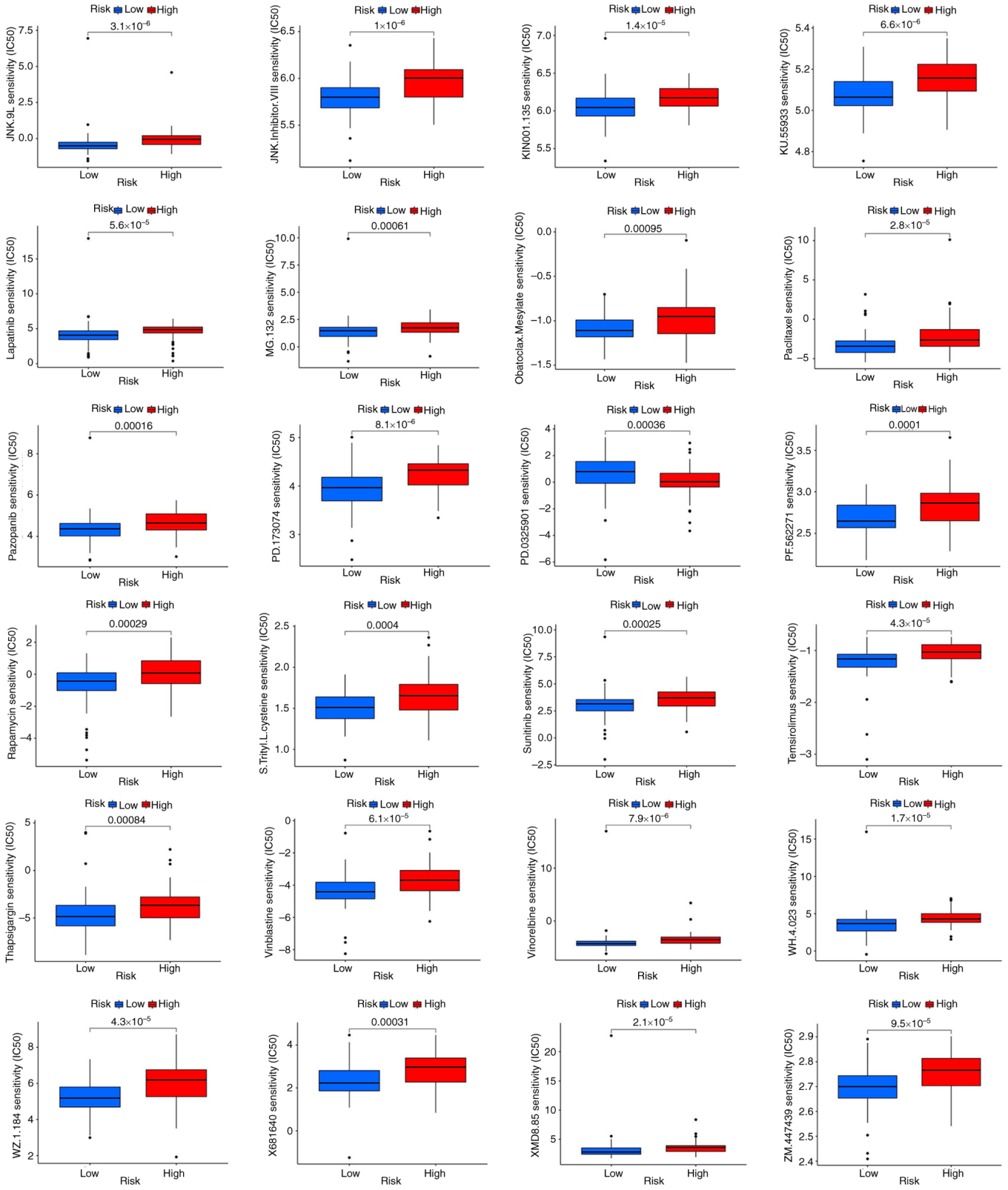

Figure 6. Differences in the tumor microenvironment between the low- and high-risk groups and prediction of potential compounds for the treatment of ESCA. (A) GSEA. (B) The ssGSEA scores of immune cells and immune functions in the risk groups. (C) The box plots of the comparison of stromal score, immune score, and ESTIMATE score, respectively, between low- and high-risk groups. (D) Expression of checkpoints in risk groups. (E) Prediction of potential compounds between the low- and high-risk groups. *P<0.05, **P<0.01, ***P<0.001. ESCA, esophageal carcinoma; GSEA, Gene Set Enrichment Analysis.

shown in Fig. 7G, the heatmap showed that the differences in immune cell infiltration in the cluster were in accordance with the analysis of immune infiltration by various platforms. Moreover, immune checkpoints, such as CD28, TNFSF14, TNFRSF14, TNFRSF14, TNFRSF9, LAIR1, HHLA2, LGALS9 and TNFSF15, were highly expressed in Cluster 3

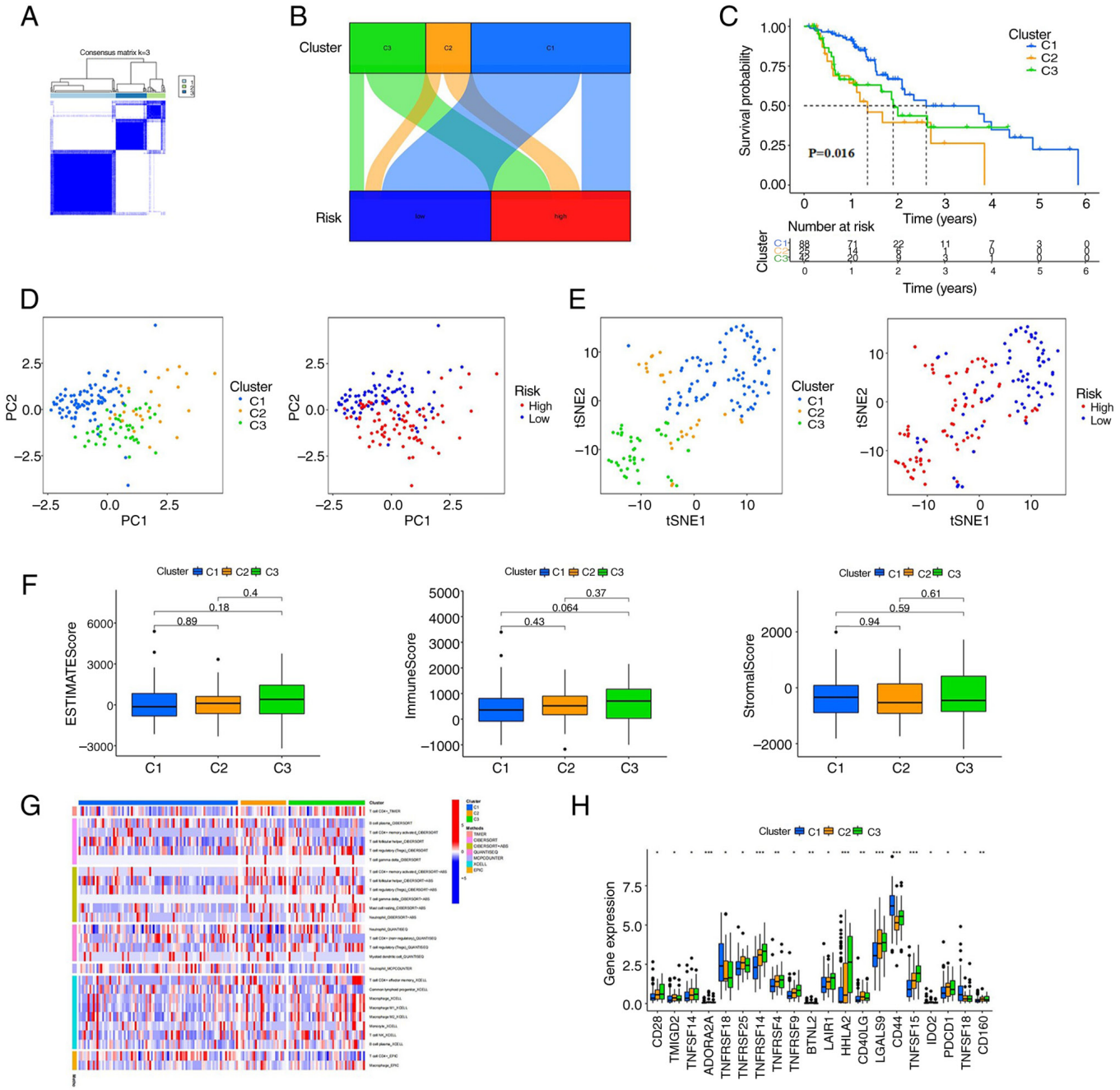

Figure 7. Continued.

(Fig. 7H). Finally, in the drug susceptibility comparison, we found 49 immunotherapeutic drugs related to systemic treatment of ESCA (Fig. 7I) by the Kruskal-Wallis test followed by Dunn's post hoc test. However, only 6 showed a significant IC50 difference between the groups.

RT-qPCR analysis. Two nrlncRNAs (LINC02811 and LINC00299) were selected and tested in various cell lines (HET-1A, KYSE150 and TE1). As shown in Fig. 8, there were significant differences in the expression levels of these lncRNAs between tumor and normal cells. All the results showed that the expression of these factors was different, which further confirmed the reliability of the risk model.

Discussion

In China, due to the lack of typical symptoms, most esophageal cancer cases are diagnosed in the middle and late stages. In recent years, its morbidity and mortality rates have been increasing. It remains a huge threat to human health (1). Multiple studies have confirmed that lncRNAs play an important role in esophageal cancer, and their functions and molecular mechanisms have been explored and emphasized. Furthermore, studies have confirmed that lncRNAs play an important indicative role in the diagnosis, treatment and prognosis evaluation of esophageal cancer, indicating that lncRNAs could be used as biomarkers and potential targets for esophageal cancer (40).

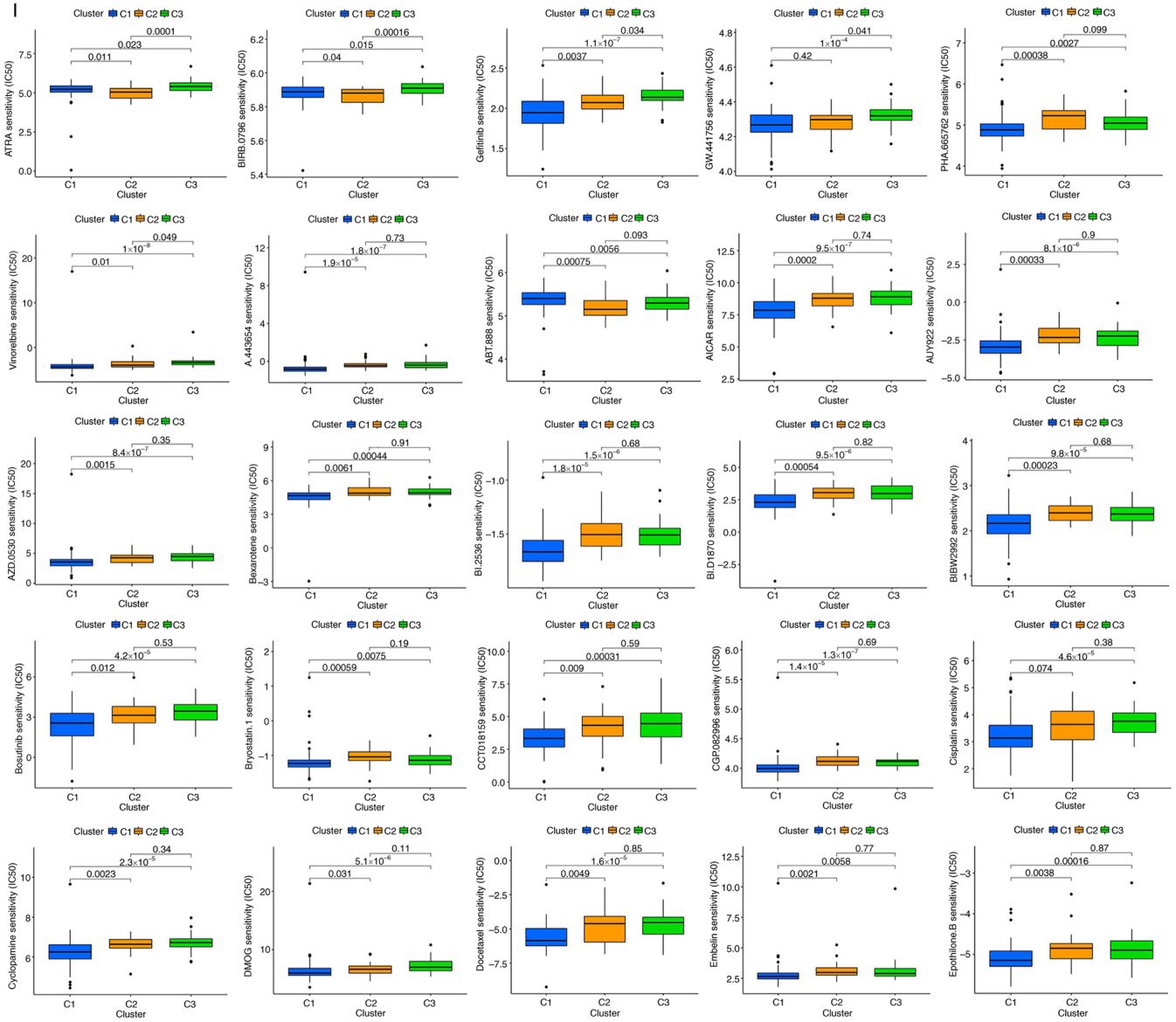

Figure 7. Continued.

LncRNAs play an important biological role in the occurrence and development of cancer. LncRNAs compete with miRNA via the competing endogenous RNA (ceRNA) mechanism or directly regulate downstream proteins. LncRNAs have been found to play these roles in esophageal cancer (41). Tang *et al* performed RNA-Seq experiments on preimmortalized human embryonic esophageal epithelial SHEE cells at passages 26 and 79 and found that LINC00885 could play a positive regulatory role in esophageal cancer (42). It is well known that lncRNAs affect not only the tumorigenesis and progression of ESCA but also the sensitivity of cancer cells to chemoradiotherapy. Therefore, reducing resistance to chemoradiotherapy by regulating lncRNA expression in ESCA patients could be regarded as a new way to enhance the therapeutic effect and prevent the development of tumors. Li *et al* (43) transplanted MALAT1-overexpressing cells into nude mice to induce tumor formation and then treated the tumors with radiotherapy. The results showed that MALAT1 overexpression could suppress radiation-induced apoptosis of tumor cells and enhance the resistance of tumor cells to radiotherapy, whereas another study reported that MALAT1 silencing could enhance the sensitivity of tumor cells to radiotherapy (44). In recent years, more studies have emphasized the key role of lncRNAs in ESCA, but the relationship between lncRNAs and ESCA has not been fully clarified and is a research hotspot.

Currently, it has been reported that the tumorigenesis and tumor progression are closely related to tumor immune function, and necroptosis has been confirmed to play an important role in this process (45,46). McComb *et al* demonstrated that necrosis-related molecules (CIAPs) effectively reduce macrophage necrosis and enhance the body's response to pathogen invasion (47). Although an increasing number of studies have shown that necroptosis is closely involved in tumorigenesis, its mechanism has not been fully elucidated. In the present study, we found that necrosis-associated lncRNAs could be used to divide patients into different subgroups, illustrating for the first time their usefulness as prognostic markers. We also systematically investigated the correlation between the tumor

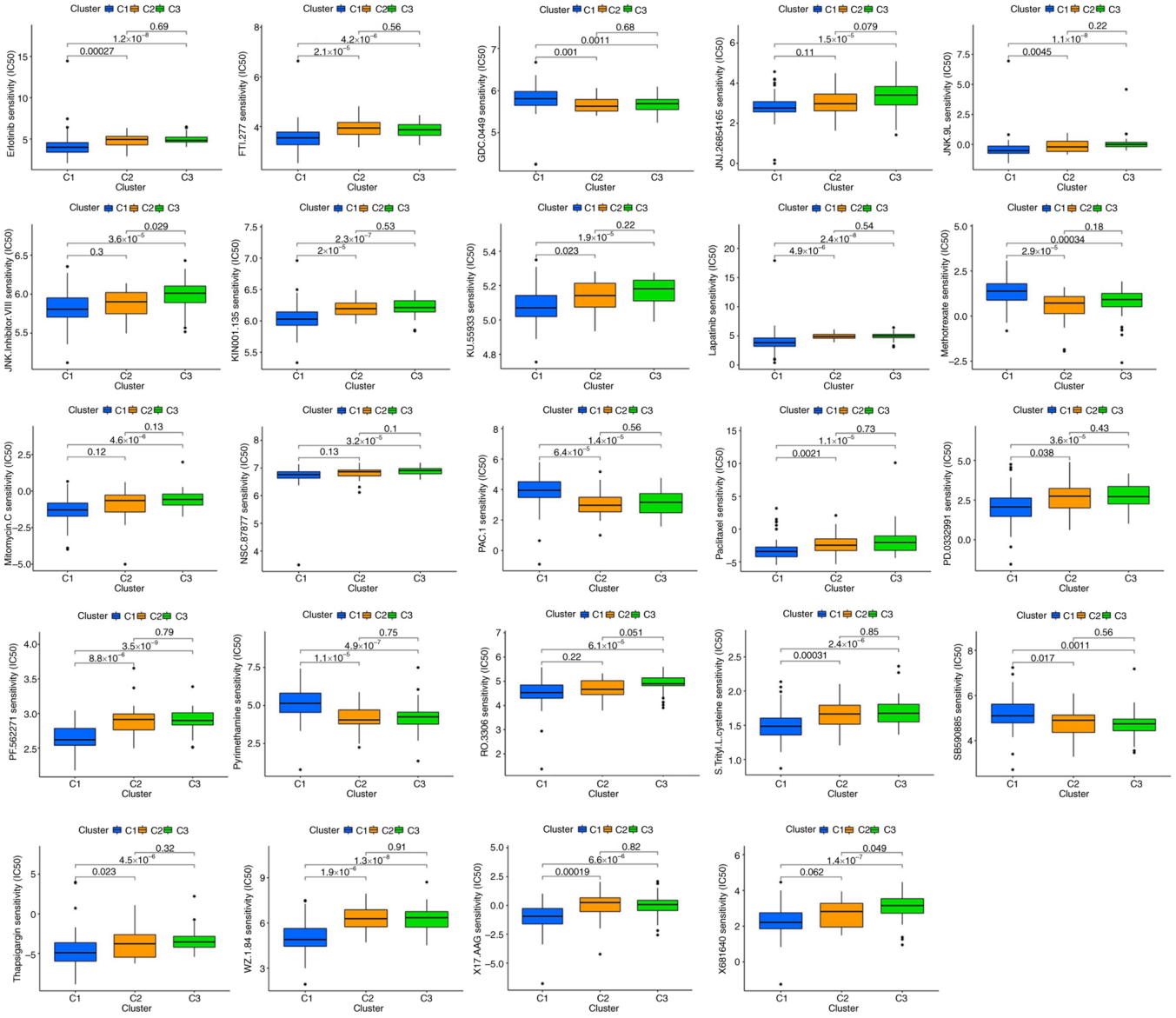

Figure 7. Cluster analysis. (A) Patients divided into three clusters. (B) Sankey diagram. (C) K-M survival curves of OS in clusters. (D) PCA of risk groups and clusters. (E) t-SNE of risk groups and clusters. (F) Box plots of the comparison of stromal score, immune score, and ESTIMATE score in clusters. (G) Heatmap of immune cells in clusters. (H) Differential expression of checkpoints in clusters. (I) Prediction of potential effective compounds for each cluster. *P<0.05, **P<0.01, ***P<0.001. K-M, Kaplan-Meier; OS, overall survival; PCA, principal component analysis; t-SNE, t-distributed Stochastic Neighbor Embedding.

microenvironment, immune cell infiltration and immune checkpoints, which is expected to be applied to clinical diagnosis and treatment in the future. We also systematically investigated the associations between the expression of these lncRNAs and tumor microenvironment features and immune checkpoint expression to assess their potential application in clinical diagnosis and treatment in the future.

Our results showed that 34 nrlncRNAs affected the survival of HNSCC patients, and 8 lncRNAs, including LINC00299, AC090912.2, AC244197.2, AL158166.1, AC079684.1, AP003696.1, LINC02811 and AC026741.1, could be used as prognostic markers. Liu *et al* identified that Linc00299 regulates the migration and proliferation of endothelial cells and vascular smooth muscle cells (VSMCs) during atherosclerosis by regulating miR-490-3p, which targets Aurora kinase A (AURKA) (48). Chang *et al* studied the role of the LINC00299/miR-135a-5p/XBP1 axis in the regulation of atherosclerosis progression, ox-LDL-induced oxidative damage, and human aortic vascular smooth muscle cell migration and invasion (49). Moreover, Manoochehri *et al* found that the occurrence of TNBC was often accompanied by hypermethylation of LINC00299 in young women, indicating a potential association between them (50). Talkowski *et al* found a functional role for these specific noncoding RNAs in brain development in subjects with LINC00299 mutations and raised the possibility that lncRNAs, as a class of abnormalities, might play an important role in human developmental disorders (51). Li *et al* suggested that LINC00299 may be an important regulator in human hypertrophic scars (HSs) that exerts its effects via its coexpressed genes (52). The other seven genes have not been further reported in the literature.

The 1-, 3-, and 5-year AUC values for the risk score model were significantly higher than those for models based on other clinical characteristics (age, sex and stage), suggesting that

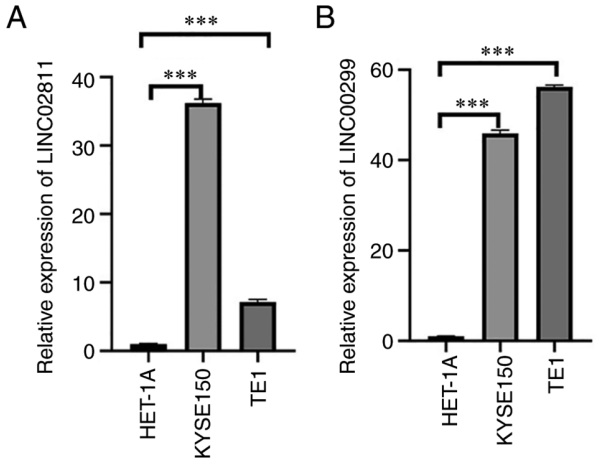

Figure 8. The RT-qPCR results of (A) LINC02811 and (B) LINC00299 expression levels in various cell lines (HET-1A, KYSE150 and TE1). The y-axes show relative expression of LINC02811 and LINC00299. ***P<0.0001. RT-qPCR, reverse transcription-quantitative polymerase chain reaction.

risk score model performs better in predicting the prognosis of ESCA patients. Cox regression analysis showed that the risk score of ESCA patients was an independent risk indicator and negatively correlated with OS. Furthermore, the correlation of a high-risk score with older age, later T and N stages and worse prognosis suggested that the risk score plays a crucial role in the classification of patient survival status. In addition, four independent factors, including risk score, age, sex and stage, were used to establish a nomogram prediction model for OS, and the calibration plots of 1-, 3-, and 5-year OS showed high consistency between the predictions and actual observations. Hence, all results indicated that the risk model is robust and an effective indicator of outcomes in ESCA patients.

In recent years, an increasing number of scholars have focused on the function and application of immune checkpoint inhibitors. Clinical trials have shown that immunotherapy strategies in ESCA patients may shift from metastatic therapy to neoadjuvant/adjuvant therapy. The addition of immunotherapy brings a good survival benefit to ESCA patients (53). Previous studies have shown that the tumor microenvironment has a significant influence on immunotherap (54,55). Immune infiltration analysis showed that CD4+ T cells and other infiltrating immune cells were more abundant in the low-risk group. Moreover, regulatory T cells (Tregs) are immunosuppressive subsets of CD4+ T cells that play an important role in maintaining self-tolerance and immune homeostasis. In tumor immunity, Tregs disrupt the immune surveillance of cancer in healthy individuals and impair the antitumor immune response of tumor-bearing hosts. Thus, this evidence suggests that Tregs accelerate the immune escape of tumor cells and further lead to various types of tumor development and progression (56). It has been demonstrated that tumor markers play an important role in ESCA by analyzing tumor immunity and immune cell levels. All results suggest that necrosis-associated lncRNAs may be associated with tumor immune infiltration. Our study predicted compounds that may be useful for the clinical treatment of diseases, which could provide a meaningful reference for future exploration of new therapeutic targets.

We divided the ESCA patients into 3 clusters, and the survival analysis showed that cluster 1 had better survival than the other groups (P=0.016). Moreover, immune checkpoints, such as CD28, TNFSF14, TNFRSF14, TNFRSF14, TNFRSF9, LAIR1, HHLA2, LGALS9 and TNFSF15, displayed higher expression in cluster 3. These analysis results suggest that these immune checkpoints are closely related to both patient prognosis and the immune microenvironment, suggesting that immunotherapy can be used as a new treatment for ESCA patients. In addition, drug susceptibility analysis results suggested that risk models and tumor subtypes could be used to guide ESCA treatment decision making.

We performed PCR verification of the selected nrlncRNAs and concluded that LINC02811 and LINC00299 were significantly differentially expressed between tumor and normal cells. Thus, they may be markers of prognosis and immune invasion in esophageal cancer. Further mechanistic research is still needed.

These studies provide meaningful references for the identification of new therapeutic targets in the future. However, there are several limitations to our study. First, all of our data came from the TCGA. Although risk profiles are valuable in assessing prognosis, there is a lack of lncRNA data from other databases and clinical information for external cohort. However, we might obtain different results by combining data from other databases. Second, we verified nrlncRNAs by cell RT-qPCR analysis, but PCR assessment of clinical samples in a future study is needed. the functions and mechanisms of these RNAs need further study. Finally, there is a lack of clinical follow-up data to confirm the value of our prognostic model. In addition, extensive clinical trials are needed to confirm the relationship between risk score and the response to immunotherapy and chemotherapy. Nevertheless, immune cell correlation analysis based on various experimental platforms can be regarded as external validation in some sense. Thus, all evidence indicates that the nrlncRNA risk model can be considered reliable and acceptable. In the future, large-scale studies should further focus on immunotherapy and chemotherapy based on bioinformatics analysis.

In this paper, we systematically evaluated the value and function of lncRNAs associated with necrosis in predicting survival, tumor microenvironment features and immune cell infiltration. We also analyzed the potential regulatory mechanisms of lncRNAs associated with necrosis, as well as the anticipated response to immunotherapy and chemotherapy agents for ESCA. Eight nrlncRNAs could predict the survival of patients with ESCA and may promote the development of personalized and precision therapies for ESCA patients. According to cell RT-qPCR analysis, LINC02811 and LINC00299 may be markers of esophageal cancer prognosis and immune invasion.

Acknowledgements

Not applicable.

Funding

This work was supported by the Medical Science Research Project of Hebei Province (grant no. 20230971).

Availability of data and materials

The datasets used and/or analyzed during the current study are available from the corresponding author on reasonable request. The RNA sequencing transcriptome data of patients with ESCA were downloaded from The Cancer Genome Atlas-ESCA dataset (https://portal.gdc.cancer.gov/).

Authors' contributions

XD, HD and JS conceived and designed the study. XD and JS confirm the authenticity of all raw data. XD, HD, MY , LL and RL downloaded and analyzed the data. XD and HD performed experiments and wrote the manuscript. XD, HD, MY, LL and RL organized the figures and tables. JS reviewed and revised the manuscript. All authors read and approved the final manuscript.

Ethics approval and consent to participate

Not applicable.

Patient consent for publication

Not applicable.

Competing interests

The authors declare that they have no competing interests.

References

1. Sung H, Ferlay J, Siegel RL, Laversanne M, Soerjomataram I, Jemal A and Bray F: Global Cancer Statistics 2020: GLOBOCAN estimates of incidence and mortality worldwide for 36 cancers in 185 countries. CA Cancer J Clin 71: 209-249, 2021.
2. Abnet CC, Arnold M and Wei WQ: Epidemiology of esophageal squamous cell carcinoma. Gastroenterology 154: 360-373, 2018.
3. Long Z, Liu W, Lin L, *et al*: Disease burden analysis of esophageal cancer in China from 1990 to 2017. Chin J Chronic Disease Prevention Control 29: 571-575, 581, 2021.
4. Li MX, Cheng WG, Chen P, *et al*: Identification and prognostic analysis of key genes in lymph node metastasis of esophageal squamous cell carcinoma. J Natural Sci Hun Normal Univ 44: 92-100, 201.
5. Short MW, Burgers KG and Fry VT: Esophageal cancer. Am Fam Physician 95: 22-28, 2017.
6. Kyle JN, Mary S and Subhasis M: Esophageal cancer: A review of epidemiology, pathogenesis, staging workup and treatment modalities. World J Gastrointest Oncol 6: 112-120, 2014.
7. Degterev A, Huang Z, Boyce M, Li Y, Jagtap P, Mizushima N, Cuny GD, Mitchison TJ, Moskowitz MA and Yuan J: Chemical inhibitor of nonapoptotic cell death with therapeutic potential for ischemic brain injury. Nat Chem Biol 1: 112-119, 2005.
8. Marshall KD and Baines CP: Necroptosis: Is there a role for mitochondria? Front Physiol 5: 323-328, 2014.
9. Declercq W, Vanden BT and Vandenabeele P: RIP kinases at the crossroads of cell death and survival. Cell 138: 229-232, 2009.
10. Krysko O, Aaes TL, Kagan VE, D'Herde K, Bachert C, Leybaert L, Vandenabeele P and Krysko DV: Necroptotic cell death in anti-cancer therapy. Immunol Rev 280: 207-219, 2017.
11. Jiao D, Cai Z, Choksi S, Ma D, Choe M, Kwon HJ, Baik JY, Rowan BG, Liu C and Liu ZG: Necroptosis of tumor cells leads to tumor necrosis and promotes tumor metastasis. Cell Res 28: 868-870, 2018.
12. Gong Y, Fan Z, Luo G, Yang C, Huang Q, Fan K, Cheng H, Jin K, Ni Q, Yu X and Liu C: The role of necroptosis in cancer biology and therapy. Mol Cancer 18: 100, 2019.
13. Snyder AG, Hubbard NW, Messmer MN, Kofman SB, Hagan CE, Orozco SL, Chiang K, Daniels BP, Baker D and Oberst A: Intratumoral acti-vation of the necroptotic pathway components RIPK1 and RIPK3potentiates anti tumor immunity. Sci Immunol 4: eaaw2004, 2019.
14. Yang Z, Jiang B, Wang Y, Ni H, Zhang J, Xia J, Shi M, Hung LM, Ruan J, Mak TW, *et al*: 2-HG inhibits necroptosis by Stim-ulating dnmt1-dependent hypermethylation of the RIP3 promoter. Cell Rep 19: 1846-1857, 2017.
15. Xu Y, Li Y, Jin J, Han G, Sun C, Pizzi MP, Huo L, Scott A, Wang Y, Ma L, *et al*: LncRNA PVT1 up-regulation is a poor prognosticator and serves as a therapeutic target in esophageal adenocarcinoma. Mol Cancer 18: 141, 2019.
16. Nugues A, ElBouazzati H, Hétuin D, Berthon C, Loyens A, Bertrand E, Jouy N, Idziorek T and Quesnel B: RIP3 is down-regulated in human myeloid leukemia cells and modulates apoptosis and caspase-mediated p65/RelA cleavage. Cell Death Dis 5: e1384, 2014.
17. Höckendorf U, Yabal M, Herold T, Munkhbaatar E, Rott S, Jilg S, Kauschinger J, Magnani G, Reisinger F, Heuser M, *et al*: RIPK3 restricts myeloid leukemogenesis by promoting cell death and differentiation of leukemia initiating Cells. Cancer Cell 30: 75-91, 2016.
18. Koo G, Morgan MJ, Lee D, Kim WJ, Yoon JH, Koo JS, Kim SI, Kim SJ, Son MK, Hong SS, *et al*: Methylation-dependent loss of RIP3 expression in cancer represses programmed necrosis in response to chemotherapeutics. Cell Re 25: 707-725, 2015.
19. Bozec D, luga AC, Roda G, Dahan S and Yeretssian G: Critical function of thenecroptosis adaptor RIPK3 in protecting from intestinal tumorigenesis. Oncotarget 7: 46384-46400, 2016.
20. Liu X, Zhou M, Mei L, Ruan J, Hu Q, Peng J, Su H, Liao H, Liu S, Liu W, *et al*: Key roles of necroptotic factors in promoting tumor growth. Oncotarget 7: 22219-22233, 2016.
21. Schmidt SV Seibert S, Walch-Ruckheim B, Vicinus B, Kamionka EM, Pahne-Zeppenfeld J, Solomayer EF, Kim YJ, Bohle RM, Smola S, *et al*: RIPK3 expression in cervical cancer cells is required for PolyIC-induced necroptosis, IL-1α release, and efficient paracrine dendritic cell activation. Oncotarget 6: 8635-8647, 2015.
22. Takemura R, Takaki H, Okada S, Shime H, Akazawa T, Oshiumi H, Matsumoto M, Teshima T and Seya T: Poly1: C-induced, TLR3 RIP3-dependent necroptosis backs up immune effector-mediated tumor elimination in vivo. Cancer Immunol Res 3: 902-914, 2015.
23. Yatim N, Jusforgues-Saklani H, Orozco S, Schulz O, Barreira da Silva R, Reis e Sousa C, Green DR, Oberst A and Albert ML: RIPKI and NF-κB signaling in dying cells determines cross-priming of $CD8^{+}$Tcells. Science 350: 328-334, 2015.
24. Kang YJ, Bang BR, Han KH, Hong L, Shim EJ, Ma J, Lerner RA and Otsuka M: Regulation of NKT cell mediated immune responses to tumours and liver inflammation by mitochondrial PGAM5-Drpl signalling. Nat Commun 6: 8371, 2015.
25. Strilic B, Yang L, Albarrán-Juárez J, Wachsmuth L, Han K, Müller UC, Pasparakis M and Offermanns S: Tumour-cell-induced endothelial cell necroptosis via death receptor 6 promotes metastasis. Nature 536: 215-218, 2016.
26. Seifert L, Werba G, Tiwari S, Giao Ly NN, Alothman S, Alqunaibit D, Avanzi A, Barilla R, Daley D, Greco SH, *et al*: The necrosome promotes pancreatic oncogenesis via CXCL1 and Mincle-induced immune suppression. Nature 532: 245-249, 2016.
27. Dragomir MP, Kopetz S, Ajani JA and Calin GA: Non-coding RNAs in GI cancers: From cancer hallmarks to clinical utility. Gut 69: 748-763, 2022.
28. Zhao Z, Liu H, Zhou X, Fang D, Ou X, Ye J, Peng J and Xu J: Necroptosis-Related lncRNAs: Predicting prognosis and the distinction between the cold and hot tumors in gastric cancer. J Oncol 2021: 6718443, 2021.
29. Xue ST, Zheng B, Cao SQ, Ding JC, Hu GS, Liu W and Chen C: Long non-coding RNA LINC00680 functions as a ceRNA to promote esophageal squamous cell carcinoma progression through the miR-423-5p/PAK6 axis. Mol Cancer 21: 69, 2022.
30. Xu JH, Chen RZ, Liu LY, Li XM, Wu CP, Zhou YT, Yan JD and Zhang ZY: LncRNA ZEB2-AS1 promotes the proliferation, migration and invasion of esophageal squamous cell carcinoma cell through miR-574-3p/HMGA2 axis. Eur Rev Med Pharmacol Sci 25: 3397, 2021.
31. Wang K, Liu F, Liu CY, An T, Zhang J, Zhou LY, Wang M, Dong YH, Li N, Gao JN, *et al*: The long noncoding RNA NRF regulates programmed necrosis and myocardial injury during ischemia and reperfusion by targeting miR-873. Cell Death Differ 23: 1394-1405, 2016.

32. Huang J, Xu Z, Teh BM, Zhou C, Yuan Z, Shi Y and Shen Y: Construction of a necroptosis-related lncRNA signature to predict the prognosis and immune microenvironment of head and neck squamous cell carcinoma. J Clin Lab Anal 36: e24480, 2022.
33. Luo L, Li L, Liu L, Feng Z, Zeng Q, Shu X, Cao Y and Li Z: A Necroptosis-Related lncRNA-Based signature to predict prognosis and probe molecular characteristics of stomach adenocarcinoma. Front Genet 13: 833928, 2022.
34. Liu L, Huang L, Chen W, Zhang G, Li Y, Wu Y, Xiong J and Jie Z: Comprehensive Analysis of Necroptosis-Related Long Noncoding RNA immune infiltration and prediction of prognosis in patients with colon cancer. Front Mol Biosci 9: 811269, 2022.
35. Chen F, Yang J, Fang M, Wu Y, Su D and Sheng Y: Necroptosis-related lncRNA to establish novel prognostic signature and predict the immunotherapy response in breast cancer. J Clin Lab Anal 36: e24302, 2022.
36. Yatim N, Jusforgues-Saklani H, Orozco S, Schulz O, Barreira da Silva R, Reis e Sousa C, Green DR, Oberst A and Albert ML: RIPK1 and NF-κB signaling in dying cells determines cross-priming of CD8 + T cells. Science 350: 328-334, 2015.
37. Zhao Z, Liu H, Zhou X, Fang D, Ou X, Ye J, Peng J and Xu J: Necroptosis-related lncRNAs: Predicting prognosis and the distinction between the cold and hot tumors in gastric cancer. J Oncol 2021: 6718443, 2021.
38. Hong W, Liang L, Gu Y, Qi Z, Qiu H, Yang X, Zeng W, Ma L and Xie J: Immune-related lncRNA to construct novel signature and predict the immune landscape of human hepatocellular carcinoma. Mol Ther Nucleic Acids 22: 937-947, 2020.
39. Geeleher P, Cox NJ and Huang RS: Clinical drug response can be predicted using baseline gene expression levels and in vitro drug sensitivity in cell lines. Genome Biology 15: R47, 2014.
40. Yang C and Chen K: Long Non-Coding RNA in esophageal cancer: A review of research progress. Pathol Oncol Res 28: 1610140, 2022.
41. Jin-Ming T and Wen-Xiang W: The role of LNCRNA ZFAS1 in esophageal Carcinoma and its mechanism. Chin J Biol: 762-768, 2020.
42. Tang D, Wang B, Khodahemmati S, Li J, Zhou Z, Gao J, Sheng W and Zeng Y: A transcriptomic analysis of malignant transformation of human embryonic esophageal epithelial cells by HPV18 E6E7. Transl Cancer Res 9: 1818-1832, 2020.
43. Li Z, Zhou Y, Tu B, Bu Y, Liu A and Kong J: Long noncoding RNA MALAT1 affects the efficacy of radiotherapy for esophageal squamous cell carcinoma by regulating Cks1 expression. J Oral Pathol Med 46: 583-590, 2017.
44. Farooqi A, Legaki E, Gazouli M, Rinaldi S and Berardi R: MALAT1 as a versatile regulator of cancer: Overview of the updates from predatory role as competitive endogenous RNA to mechanistic insights. Curr Cancer Drug Targets: Jul 30, 2020. doi: 10.2174/1568009620999200730183110 (Epub ahead of print).
45. Seifert L, Werba G, Tiwari S, Giao Ly NN, Alothman S, Alqunaibit D, Avanzi A, Barilla R, Daley D, Greco SH, *et al*: The necrosome promotes pancreatic oncogenesis via CXCL1 and Mincle-Induced immune suppression. Nature 532: 245-249, 2016.
46. Snyder AG, Hubbard NW, Messmer MN, Kofman SB, Hagan CE, Orozco SL, Chiang K, Daniels BP, Baker D and Oberst A: Intratumoral activation of the necroptotic pathway components RIPK1 and RIPK3 potentiates antitumor immunity. Sci Immunol 4: eaaw2004, 2019.
47. McComb S, Cheung HH, Korneluk RG, Wang S, Krishnan L and Sad S: cIAP1 and cIAP2 limit macrophage necroptosis by inhibiting Rip1and Rip3 activation. Cell Death Differ 19: 1791-1801, 2012.
48. Liu Y, Chen Y, Tan L, Zhao H and Xiao N: Linc00299/miR-490-3p/AURKA axis regulates cell growth and migration in atherosclerosis. Heart Vessels 34: 1370-1380, 2019.
49. Chang M, Liu G, Wang Y, Lv H and Jin Y: Long non-coding RNA LINC00299 knockdown inhibits ox-LDL-induced T/G HA-VSMC injury by regulating miR-135a-5p/XBP1 axis in atherosclerosis. Panminerva Med 64: 38-47, 2022.
50. Manoochehri M, Jones M, Tomczyk K, Fletcher O, Schoemaker MJ, Swerdlow AJ, Borhani N and Hamann U: DNA methylation of the long intergenic noncoding RNA 299 gene in triple-negative breast cancer: Results from a prospective study. Sci Rep 10: 11762, 2020.
51. Talkowski ME, Maussion G, Crapper L, Rosenfeld JA, Blumenthal I, Hanscom C, Chiang C, Lindgren A, Pereira S, Ruderfer D, *et al*: Disruption of a large intergenic noncoding RNA in subjects with neurodevelopmental disabilities. Am J Hum Genet 91: 1128-1134, 2012.
52. Li M, Wang J, Liu D and Huang H: High throughput sequencing reveals differentially expressed lncRNAs and circRNAs, and their associated functional network, in human hypertrophic scars. Mol Med Rep 18: 5669-5682, 2018.
53. Kakeji Y, Oshikiri T, Takiguchi G, Kanaji S, Matsuda T, Nakamura T and Suzuki S: Multimodality approaches to control esophageal cancer: Development of chemoradiotherapy, chemotherapy, and immunotherapy. Esophagus 18: 25-32, 2021.
54. Frankel T, Lanfranca MP and Zou W: The role of tumor microenvironment in cancer immunotherapy. Adv Exp Med Biol 1036: 51-64, 2017.
55. Pitt JM, Marabelle A, Eggermont A, Soria JC, Kroemer G and Zitvogel L: Targeting the tumor microenvironment: Removing obstruction to anticancer immune responses and immunotherapy. Ann Oncol 27: 1482-1492, 2016.
56. Nishikawa H and Koyama S: Mechanisms of regulatory T cell infiltration in tumors: Implications for innovative immune precision therapies. J Immunother Cancer 9: e002591, 2021.